

# Growth, Structure, and Properties of Single Crystals of SrBPO<sub>5</sub>

Shilie Pan,<sup>†</sup> Yicheng Wu,<sup>\*,†</sup> Peizhen Fu,<sup>†</sup> Guochun Zhang,<sup>†</sup> Zhihua Li,<sup>†</sup>  
Chenxia Du,<sup>‡</sup> and Chuangtian Chen<sup>†</sup>

Beijing Center for Crystal R&D, Technical Institute of Physics and Chemistry,  
Chinese Academy of Sciences, Beijing 100080, China, and Chemistry Department,  
Zhengzhou University, Zhengzhou, Henan 450052, China

Received September 13, 2002. Revised Manuscript Received March 24, 2003

Single crystals of strontium borophosphate, SrBPO<sub>5</sub>, have been grown with sizes up to 25 × 15 × 10 mm<sup>3</sup> from the BPO<sub>4</sub> flux by the top-seeded solution growth method. The compound crystallizes in the trigonal system, space group *P*3<sub>2</sub>21 (No. 154), with *a* = 6.8850(10) Å, *c* = 6.8700(14) Å, and three formula units per cell. The SrBPO<sub>5</sub> compound is built up of infinite anionic units of BO<sub>4</sub> and PO<sub>4</sub> tetrahedra joined by common vertexes. It contains single chains of BO<sub>4</sub> tetrahedra running parallel to [001], which are linked to terminal PO<sub>4</sub> tetrahedra to form spiral chains. The ultraviolet transmission spectrum of SrBPO<sub>5</sub> crystals was reported. The refractive indices were measured by the minimum deviation technique and fitted to the Sellmeier equations. The crystal exhibits an optical second-harmonic generation effect similar to that of KDP (KH<sub>2</sub>PO<sub>4</sub>).

## Introduction

In recent years there has been considerable progress in the development of coherent sources based on nonlinear optical (NLO) processes in borate crystals.<sup>1–6</sup> The success of these crystals can be attributed to the unique structural characteristics of boron–oxygen groups. In addition, the phosphates, such as KTiOPO<sub>4</sub> and KH<sub>2</sub>PO<sub>4</sub>, have also been widely used in electro-optical applications such as frequency conversions in laser spectroscopy.<sup>7,8</sup> Considering the excellent properties of borates and phosphates, we expect that the combination of the borate and the phosphate group in the same crystal may generate a whole new class of NLO materials. Until now, there have been few materials that contain both the borate group and the phosphate group.<sup>9</sup> The extensive search in borophosphates led to the finding of a new NLO crystal, SrBPO<sub>5</sub>.

The SrBPO<sub>5</sub> compound was first prepared by Bauer.<sup>10</sup> The powder second-harmonic intensities of subsolidus

phase state of borosilicates, borogermanates, and borophosphates with stillwellite-like structure were reported to the same order magnitude as crystalline quartz.<sup>11</sup> The crystal structure of SrBPO<sub>5</sub> has been resolved from powder data using the Rietveld method in the space group *P*3<sub>1</sub>21.<sup>12</sup> It is worthy to note that the *c* parameter of SrBPO<sub>5</sub> according to data<sup>12</sup> should be 2 times smaller as compared with that reported in the reference.<sup>10</sup> Apart from that, further understanding of the relationship between the structure and the properties of SrBPO<sub>5</sub> prompted us to reinvestigate the crystal structure of SrBPO<sub>5</sub> using the single-crystal X-ray diffraction technique. The growth of crystals large enough for the measurements of linear and nonlinear optical properties has not been reported in the literature. In this paper, we describe the synthesis, crystal growth, structure, and linear and nonlinear optical properties of SrBPO<sub>5</sub> crystals.

## Experimental Section

**Synthesis and Crystal Growth.** Polycrystalline samples of SrBPO<sub>5</sub> were prepared by using solid-state reaction techniques. The stoichiometric mixture of SrCO<sub>3</sub>, H<sub>3</sub>BO<sub>3</sub>, and NH<sub>4</sub>H<sub>2</sub>PO<sub>4</sub> (all of analytical grade) was ground thoroughly in an agate mortar and then packed into a platinum crucible. The temperature was raised to 500 °C at a rate of 2 °C/min to avoid ejection of powdered raw material from the crucible due to vigorous evolution of CO<sub>2</sub>, NH<sub>3</sub>, and decomposition of H<sub>3</sub>BO<sub>3</sub>. After preheating at 500 °C for 10 h, the products were cooled to room temperature and ground up again; the mixture was heated at 900 °C for 24 h and then cooled to room temperature. The purity of the sample was checked by X-ray powder diffraction. A single-phase powder of SrBPO<sub>5</sub> was

\* To whom correspondence should be addressed. E-mail: ycwu@cl.cryo.ac.cn.

<sup>†</sup> Chinese Academy of Sciences.

<sup>‡</sup> Zhengzhou University.

(1) Chen, C.; Wu, B.; Jiang, A.; You, G. *Sci. Sin.* **1985**, *B28*, 235.

(2) Chen, C.; Wu, Y.; Jiang, A.; You, G.; Li, R.; Lin, S. *J. Opt. Soc. Am.* **1989**, *B6*, 616.

(3) Wu, Y.; Sasaki, T.; Nakai, S.; Yokotani, A.; Tang, H.; Chen, C. *Appl. Phys. Lett.* **1993**, *62*, 2614.

(4) Mei, L.; Chen, C.; Wu, B. *J. Appl. Phys.* **1993**, *74*, 7014.

(5) Chen, C.; Wang, Y.; Wu, B.; Wu, K.; Zeng, W.; Yu, L. *Nature* **1995**, *373*, 322.

(6) Sasaki, T.; Kuroda, I.; Nakajima, S.; Yamaguchi, K.; Watanabe, S.; Mori, Y.; Nakai, S. *Proceedings on Advanced Solid-State Laser Conference*; Optical Society of America: Washington, D.C., 1995; Vol. 24, p 91.

(7) Liu, Y. S.; Dentz, D.; Belt, R. *Opt. Lett.* **1983**, *9*, 76.

(8) Bass, M.; Barrett, H. H. *Appl. Opt.* **1973**, *12*, 690.

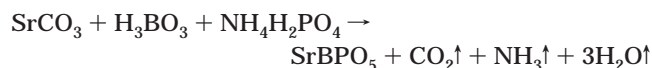
(9) Wu, Y.; Wang, G.; Fu, P.; Liang, X.; Xu, Z.; Chen, C. In *Abstract Book of The 1<sup>st</sup> Asian Conference on Crystal Growth and Crystal Technology*, Sendai, Japan, 2000, p 113. This paper was later published in *J. Cryst. Growth* **2001**, *229*, 205.

(10) Bauer, H. Z. *Anorg. Allg. Chem.* **1965**, *337*, 183.

(11) Stefanovich, S. Yu.; Sigaev, V. N.; Dechev, A. V.; Mosunov, A. V. *Zh. Neorg. Khim.* **1995**, *40*, 1729.

(12) Kniep, R.; Gozel, G.; Eisenmann, B.; Rohr, C.; Asbrand, M.; Kizilyalli, M. *Angew. Chem., Int. Ed. Engl.* **1994**, *33*, 749.

obtained when repeated heat treatment caused no further changes in the X-ray powder diffraction. The chemical equation can be expressed as follows:



The crystal was grown using BPO<sub>4</sub> as the flux. In the first run of growth, a platinum wire was dipped into the solution, and the temperature was reduced at a rate of 1 °C/h. The obtained crystals were cracked, but parts of them were usable as seeds.

To grow large SrBPO<sub>5</sub> crystals, the main efforts have focused on the top-seeded solution growth method. A platinum crucible containing the crystal growth charge was put into the furnace. The furnace was heated rapidly to 1090 °C and maintained for 24 h, and then it was cooled rapidly to 990 °C. A seed crystal of SrBPO<sub>5</sub> attached to a platinum rod was inserted slowly into the crucible and kept in contact with the surface of the solution, while a temperature of 990 °C was maintained for half an hour to dissolve the outer surface of the seed. The growing crystal was rotated at a rate of 20 rpm. The solution was then cooled rapidly to the saturation temperature of 985 °C determined by repeated seeding, and then the temperature was slowly reduced to 910 °C at a rate of 0.5–1.5 °C/day until the end of the growth. The crystal thus obtained was drawn out of the solution surface, cooled to room temperature at a rate of 30 °C/h, and then slowly taken out from the furnace.

**X-ray Crystallography.** X-ray powder diffraction analysis for SrBPO<sub>5</sub> was performed with a Bruker D8 ADVANCE X-ray diffractometer with Cu K $\alpha$  radiation. The crystal structure of SrBPO<sub>5</sub> was investigated by using a Rigaku-Raxis-IV imaging plate equipped with graphite monochromated Mo K $\alpha$  radiation. The systematic extinction of the reflection shows that the possible space groups were *P*<sub>3</sub>21 and *P*<sub>3</sub>21; we preferred *P*<sub>3</sub>21 because the final *R* factor of 0.0482 by 408 observed reflections [*I* > 2 $\sigma$ (*I*)] for *P*<sub>3</sub>21 is smaller than that of 0.0658 for *P*<sub>3</sub>21. In contrast, the space group of CaBPO<sub>5</sub> and BaBPO<sub>5</sub> reported in the literature using the Rietveld method is *P*<sub>3</sub>21.<sup>12,13</sup> The experimental parameters for data collection and refinement are given in Table 1. The intensity data were corrected for Lorentz-polarization factors. An empirical absorption correction was applied to all observed reflections. The structure was solved with SHELXS-97<sup>14</sup> by the direct method and refined with SHELXL-97<sup>15</sup> by full-matrix least-squares techniques with anisotropic thermal parameters for all atoms. The final refined atomic positions and isotropic thermal parameters are given in Table 2. The main interatomic distances are listed in Table 3.

**Ultraviolet Spectrum Measurement.** The transmittance spectrum of SrBPO<sub>5</sub> was recorded at room temperature using a Perkin-Elmer Lambda 900 UV/Vis/NIR spectrophotometer, which can operate over the range 175–3000 nm.

**Second-Harmonic Generation Measurement.** The measurement of the powder frequency-doubling effect was carried out on the SrBPO<sub>5</sub> sample by means of the method of Kurtz and Perry.<sup>16</sup> The fundamental wavelength is 1064 nm generated by a Q-switched Nd:YAG laser. The SHG wavelength is 532 nm. KDP powder was used as a reference to assume the effect.

## Results and Discussion

Since SrBPO<sub>5</sub> melts incongruently,<sup>10</sup> the flux method is necessary for the purpose of its crystal growth. The

**Table 1. Crystal Data and Structure Refinement**

empirical formula	SrBPO <sub>5</sub>
temperature	291(2) K
wavelength	0.71073 Å
crystal system	trigonal
space group	<i>P</i> <sub>3</sub> 21
unit cell dimensions	<i>a</i> = 6.8850(10) Å $\alpha$ = 90° <i>b</i> = 6.8850(10) Å $\beta$ = 90° <i>c</i> = 6.8700(14) Å $\gamma$ = 120°
volume	282.03(8) Å <sup>3</sup>
<i>Z</i>	3
density (calculated)	3.699 g/cm <sup>3</sup>
absorption coefficient	14.657 /mm
<i>F</i> (000)	294
crystal size	0.15 × 0.10 × 0.10 mm <sup>3</sup>
$\theta$ range for data collection	3.42–27.19°
index ranges	0 ≤ <i>h</i> ≤ 8, −8 ≤ <i>k</i> ≤ 7, −8 ≤ <i>l</i> ≤ 8
reflections collected	1023
independent reflections	415 [ <i>R</i> (int) = 0.1105]
completeness to $\theta$ = 27.19	98.1%
absorption correction	empirical
max. and min. transmission	0.3219 and 0.2172
refinement method	full-matrix least-squares on <i>F</i> <sup>2</sup>
data/restraints/parameters	415/0/40
goodness-of-fit on <i>F</i> <sup>2</sup>	1.161
final <i>R</i> indices [ <i>I</i> > 2 $\sigma$ ( <i>I</i> )]	<i>R</i> 1 = 0.0482, <i>wR</i> 2 = 0.1218
<i>R</i> indices (all data)	<i>R</i> 1 = 0.0499, <i>wR</i> 2 = 0.1236
absolute structure parameter	0.23(4)
extinction coefficient	0.28(3)
largest diff. peak and hole	1.495 and −0.988 e Å <sup>−3</sup>

**Table 2. Atomic Coordinates (×10<sup>4</sup>) and Equivalent Isotropic Displacement Parameters (Å<sup>2</sup> × 10<sup>3</sup>) for SrBPO<sub>5</sub>; *U*<sub>Eq</sub> Is Defined as One-Third of the Trace of the Orthogonalized *U*<sub>*ij*</sub> Tensor**

atom	<i>x</i>	<i>y</i>	<i>z</i>	<i>U</i> <sub>eq</sub>
Sr(1)	3950(2)	0	1667	7(1)
P(1)	4051(4)	0	−3333	5(1)
B(1)	8990(20)	0	1667	9(2)
O(1)	5500(11)	4122(11)	1436(7)	12(1)
O(2)	6624(9)	−1884(9)	1275(8)	9(2)
O(3)	444(12)	444(12)	0	12(2)

**Table 3. Selected Bond Lengths (Å) for SrBPO<sub>5</sub><sup>a</sup>**

atoms	distances	atoms	distances
Strontium Polyhedron		Boron Tetrahedron	
Sr(1)–O(1)#1	2.488(6)	B(1)–O(3)#11	1.451(10)
Sr(1)–O(1)	2.488(6)	B(1)–O(3)	1.451(10)
Sr(1)–O(1)#2	2.720(5)	B(1)–O(2)	1.513(11)
Sr(1)–O(1)#3	2.720(5)	B(1)–O(2)#1	1.513(11)
Sr(1)–O(2)#1	2.744(6)	mean	1.482(10)
Sr(1)–O(2)	2.744(6)	Phosphorus Tetrahedron	
Sr(1)–O(3)#4	2.823(3)	P(1)–O(1)#3	1.504(6)
Sr(1)–O(3)#5	2.823(3)	P(1)–O(1)#8	1.504(6)
Sr(1)–O(2)#6	2.857(6)	P(1)–O(2)#7	1.586(6)
Sr(1)–O(2)#7	2.857(6)	P(1)–O(2)#9	1.586(6)
mean	2.726(5)	mean	1.545(6)

<sup>a</sup> Symmetry transformations used to generate equivalent atoms: (#1) *x* − *y*, −*y*, −*z* + 1/3; (#2) −*x* + 1, −*x* + *y*, −*z* + 2/3; (#3) −*y* + 1, *x* − *y*, *z* − 1/3; (#4) −*x* + *y* + 1, −*x* + 1, *z* + 1/3; (#5) *x* − 1, *y*, *z*; (#6) −*x* + 1, −*x* + *y* + 1, −*z* + 2/3; (#7) −*y*, *x* − *y* − 1, *z* − 1/3; (#8) −*x* + *y* + 1, −*x*, *z* + 1/3; (#9) −*y* + 1, *x* − *y* − 1, *z* − 1/3; (#10) *x* + 1, *y*, *z*; (#11) −*x* + *y* + 2, −*x* + 1, *z* + 1/3; (#12) −*x* + 1, −*x* + *y*, −*z* − 1/3; (#13) −*x* + 1, −*x* + *y* + 1, −*z* − 1/3; (#14) *x*, *y*, *z* − 1.

success of growth depends to a large extent on whether an appropriate flux can be found. For this reason, efforts have been made to search for the suitable flux to grow SrBPO<sub>5</sub> crystals. According to the choice rules of fluxes, if a surplus of constituents of the compounds can act as the flux for the growth of the crystals of that compound, it will be possible to prevent the flux from contaminating the grown crystal. The crystals grown in such a solution will be of high purity and good quality. So several self-

(13) Shi, Y.; Zhang, H.; Liu, Q.; Chen, X.; Yang, J.; Zhuang W.; Rao, G. *J. Solid State Chem.* **1998**, *135*, 43.

(14) Sheldrick, G. M. *SHELXS-97: Program for the solution of Crystal Structure*; University of Göttingen: Göttingen, Germany, 1997.

(15) Sheldrick, G. M. *SHELXL-97: Program for crystal structures refinement*; University of Göttingen: Göttingen, Germany, 1997.

(16) Kurtz, S. W.; Perry, T. T. *J. Appl. Phys.* **1968**, *39*, 3798.

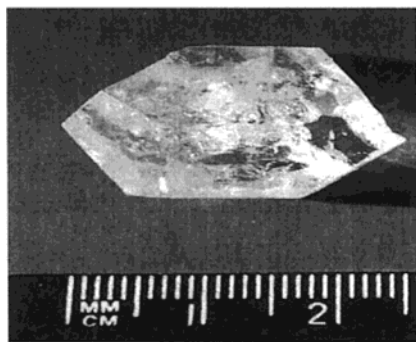


**Figure 1.** Photograph of SrBPO<sub>5</sub> crystal with use of the top-seeded solution growth method.

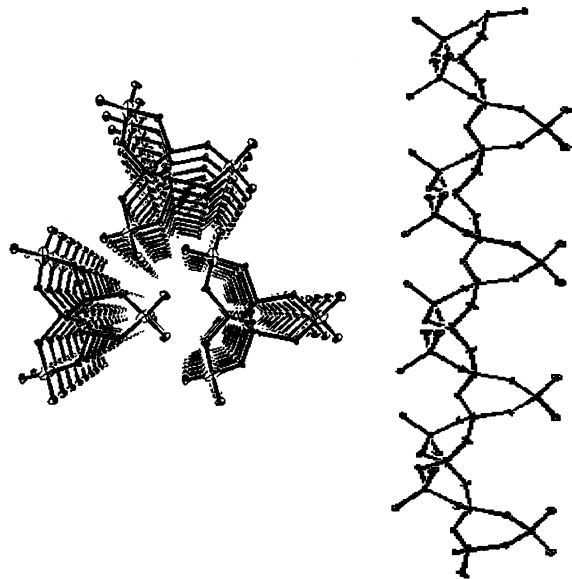


**Figure 2.** Section of the crystal structure of SrBPO<sub>5</sub>. Left: Packing of the chains along [001]. Right: Infinite chains running parallel to [001].

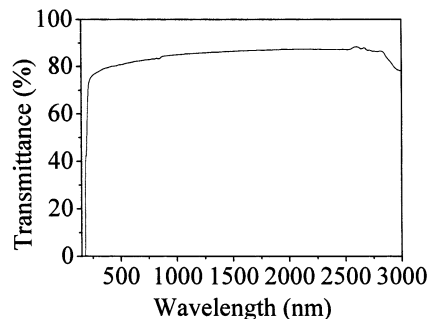
fluxes were first investigated for growing SrBPO<sub>5</sub>, such as SrCO<sub>3</sub>, H<sub>3</sub>BO<sub>3</sub>, and NH<sub>4</sub>H<sub>2</sub>PO<sub>4</sub>. The results indicate that the BPO<sub>4</sub> (H<sub>3</sub>BO<sub>3</sub>:NH<sub>4</sub>H<sub>2</sub>PO<sub>4</sub>=1:1) flux system is more suitable than others. Several ratios of SrBPO<sub>5</sub>:BPO<sub>4</sub> were tested for growing SrBPO<sub>5</sub> crystals. When a wider crystallization zone and higher crystal yield are taken into account, the suitable molar ratios of SrBPO<sub>5</sub>:BPO<sub>4</sub> for the growth of SrBPO<sub>5</sub> crystals turned out to be 1:0.7. A SrBPO<sub>5</sub> crystal with dimensions of 25 × 15 × 10 mm<sup>3</sup> was grown under this condition. Figure 1 shows the SrBPO<sub>5</sub> crystal by the top-seeded solution growth method using BPO<sub>4</sub> as the flux. It shows that the obtained crystal is colorless and partially transparent and the crystal exhibits fairly distinguishable facets.

Figure 2 represents a view of the structure of SrBPO<sub>5</sub>. Similarly to CaBPO<sub>5</sub> and BaBPO<sub>5</sub>,<sup>12,13</sup> SrBPO<sub>5</sub> belongs to the stillwellite structural type.<sup>17</sup> It is built up of infinite anionic units of BO<sub>4</sub> and PO<sub>4</sub> tetrahedra joined by common vertexes. The SrBPO<sub>5</sub> compound contains single chains of BO<sub>4</sub> tetrahedra running parallel to [001], which are linked to terminal PO<sub>4</sub> tetrahedra to form spiral chains. The "molecular" motif that repeats along the chain is BPO<sub>7</sub>, in which four of the O atoms

**Table 4. Bond Valence Analysis of the SrBPO<sub>5</sub><sup>18 a</sup>**

atom	O1	O2	O3	Σ <sub>cations</sub>
Sr	0.368 <sup>[×2]</sup> + 0.197 <sup>[×2]</sup>	0.184 <sup>[×2]</sup> + 0.136 <sup>[×2]</sup>	0.149 <sup>[×2]</sup>	2.068
P	1.310 <sup>[×2]</sup>	1.050 <sup>[×2]</sup>		4.720
B		0.681 <sup>[×2]</sup>	0.806 <sup>[×2]</sup>	2.974
Σ <sub>anions</sub>	1.875	2.051	1.910	

<sup>a</sup> Left and right superscripts indicate the number of equivalent bonds for anions and cations, respectively.



**Figure 3.** Transmission spectrum of SrBPO<sub>5</sub> crystals.

are shared in repeating this motif to give the formulation BPO<sub>3</sub>O<sub>4/2</sub> ≡ BPO<sub>5</sub>. The spiral chains, screwing along the 3<sub>2</sub> axis, provide the linkage between the columns composed of Sr 10-fold polyhedra. The bond valence sums of each atom in the compound SrBPO<sub>5</sub> are calculated using the relation proposed by Brese and O'Keefe<sup>18</sup> and listed in Table 4.

Optical properties were measured on a single crystal, samples 2 mm in thickness cut from the as-grown crystals and then polished on diamond-impregnated laps. The transmittance spectrum was recorded with the (100) face as the incident surface. Figure 3 shows the transmission spectrum of SrBPO<sub>5</sub> crystals. It can be seen that a wide transmission range is observed in the UV to IR region from 180 to 3000 nm with the UV absorption edge at about 180 nm. SrBPO<sub>5</sub> has a wider transparency region than KDP. There are no absorption peaks in the whole range of the spectrum, but the transmission intensity sharply decreases from 210 nm and reaches zero at about 180 nm.

Measurements of refractive indices and determination of Sellmeier equations in the range that is accessible for frequency doubling are needed for further prediction of the shortest SHG wavelength and the phase-matching directions.<sup>19</sup> The refractive index dispersion of SrBPO<sub>5</sub> was determined by the minimum deviation technique at 15 different wavelengths between 404.7 and 1514.3 nm. Since SrBPO<sub>5</sub> is a uniaxial crystal with point group symmetry *P*3<sub>2</sub>21, it is possible to measure both *n*<sub>o</sub> and *n*<sub>e</sub> using a prism cut with the edge at the apex parallel to the crystallographic *c*-axis and the (100) face as the incident surface. The incident polarized beam is perpendicular to the (100) incident surface, *n*<sub>e</sub> and *n*<sub>o</sub> are the refractive indices of light polarized parallel and perpendicular to the optical axis (crystallographic *c*-axis), respectively. The values of room-temperature refractive indices for both the ordinary and extraordinary polarizations measured at specific wavelengths are summarized in Table 5. The Sellmeier equations, which

(17) Voronkov, A. A.; Pyatenko, Yu. A. *Sov. Phys. Crystallogr.* **1967**, *12*, 214.

(18) Brese, N. E.; O'Keefe, M. *Acta Crystallogr.* **1991**, *B47*, 192.  
 (19) Fan, T. Y.; Huang, C. E.; Hu, B. Q.; Eckardt, R. C.; Fan, Y. X.; Byer, R. L.; Feigelson, R. S. *Appl. Opt.* **1987**, *26*, 2390.

**Table 5. Refractive Indices of the SrBPO<sub>5</sub> Crystal**

$\lambda$ ( $\mu\text{m}$ )	$n_o$			$n_e$		
	exptl	calcd	errors	exptl	calcd	errors
0.4047	1.64997	1.65036	-0.00039	1.67013	1.67048	-0.00035
0.4358	1.64606	1.64609	-0.00003	1.66593	1.66603	-0.00010
0.4861	1.64134	1.64116	0.00018	1.66103	1.66084	0.00019
0.4916	1.64089	1.64072	0.00017	1.66053	1.66038	0.00015
0.5461	1.63729	1.63716	0.00013	1.65670	1.65659	0.00011
0.5780	1.63565	1.63555	0.00010	1.65493	1.65487	0.00006
0.5893	1.63509	1.63504	0.00005	1.65443	1.65432	0.00011
0.6563	1.63247	1.63254	-0.00007	1.65156	1.65162	-0.00006
0.6943	1.63121	1.63140	-0.00019	1.65024	1.65040	-0.00016
0.8072	1.62882	1.62876	0.00006	1.64765	1.64753	0.00012
0.8617	1.62775	1.62774	0.00001	1.64627	1.64641	-0.00014
0.9592	1.62599	1.62615	-0.00016	1.64459	1.64467	-0.00008
1.0680	1.62442	1.62459	-0.00017	1.64283	1.64296	-0.00013
1.2564	1.62304	1.62211	0.00093	1.64126	1.64022	0.00104
1.5143	1.61856	1.61876	-0.00020	1.63629	1.63652	-0.00023

are fitted with the above-measured refractive indices, are as follows:

$$n_o^2 = 2.70414 + 0.01185505/(\lambda^2 - 0.02995851) - 0.01359747\lambda^2$$

$$n_e^2 = 2.64339 + 0.01072471/(\lambda^2 - 0.03341188) - 0.01210005\lambda^2$$

where  $\lambda$  is the wavelength expressed in micrometers. The values calculated from them are consistent with experimental ones to the third decimal place. Figure 4 shows the measured and fitted refractive index data for both  $n_o$  and  $n_e$ .

The Sellmeier equations predict that the shortest SHG wavelength for the crystal is 397.5 nm for type I phase matching, so the SHG of a Nd:YAG laser radiation (1064 nm) is possible for type I phase matching. The phase matching angle for type I SHG of 1064 nm calculated from the Sellmeier equations is 37.6°.

The compound crystallizes in a non-centro-symmetric space group, a basic condition for a potential harmonic generation material. According to the literature reported,<sup>20</sup> the nonlinearity of a borate crystal originates in the boron–oxygen groups; borates containing BO<sub>4</sub>

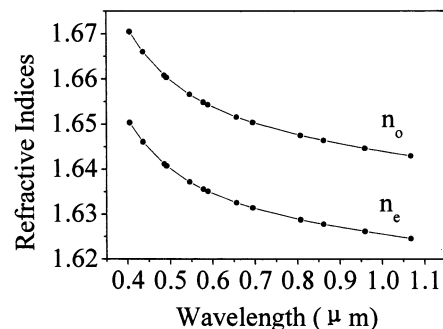


**Figure 4.** Refractive index dispersion curves of SrBPO<sub>5</sub> crystal. The points are experimental values; curves are the fits given by the Sellmeier equation.

groups could possess a SHG effect smaller than that containing BO<sub>3</sub> groups. In fact, the experiment showed that green light was observed and its intensity was about as large as that of KDP when the crystal grown from the top-seeded solution growth method was ground into powder and loaded into a quartz cell. It means that the powder nonlinear optical effect of SrBPO<sub>5</sub> is about the same as that of KDP, which originates from PO<sub>4</sub> groups. Therefore, it is considered that the main nonlinearity of SrBPO<sub>5</sub> originates from PO<sub>4</sub> groups and very limited from BO<sub>4</sub> groups.

The SrBPO<sub>5</sub> crystal presents good mechanical properties for easy cutting and polishing. Its hardness is 6.0 MΩ, close to that of quartz. The crystal is chemically stable and is not hygroscopic.

In conclusion, SrBPO<sub>5</sub> has been successfully grown by the top-seeded solution growth method using BPO<sub>4</sub> as the flux and its crystal structure has been studied. Its main structural elements are spiral chains and the “molecular” motif that repeats along the chain is BPO<sub>7</sub>. SrBPO<sub>5</sub> crystal is transparent down to 180 nm. The Sellmeier equations predict that the SHG of Nd:YAG laser radiation (1064 nm) is possible for type I phase matching. The SHG effect of SrBPO<sub>5</sub> is similar to that of KDP.

**Acknowledgment.** This work was supported by the National Fundamental Key Research Program of China.

CM020878K

(20) Chen, C.; Wu, Y.; Li, R. *Int. Rev. Phys. Chem.* **1989**, *8*, 65.